A Versatile Data Acquisition System for Goldstone

M. S. Reid and R. A. Gardner
Communications Elements Research Section

A versatile data acquisition system has been provided at Goldstone. It is capable of recording a wide variety of parameters from widely separated geographical locations with varying integration times and recording speeds. It is fast, accurate, and modular in form so that it can be readily expanded. This article describes the data system, discusses accuracies, and gives examples of data recorded with the system's capability of operation with preprocessing.

I. Introduction

A data acquisition system designated Solar and Microwave Data Acquisition System (SMDAS) has been designed, built, and implemented at the Venus Station (DSS 13) at Goldstone. This system is used for the acquisition of microwave data for the atmospheric radio propagation program (Refs. 1 and 2), solar energy data for the solar energy instrumentation program (Ref. 3), and meteorological data for the use of both of these projects. The data system has been designed for maximum flexibility in type of data, number of channels, location of sensors and speed of recording. Maximum flexibility of operation has also been a design consideration so that the response time for the inclusion of new or additional experimental data is minimal. This article describes the SMDAS, discusses accuracy of recording, and gives examples of recorded data.

II. System Description

The system consists of a central station, housed in a standard electronics rack, and up to ten remote stations. The remote stations are housed in environmental enclosures which can withstand extremes of ambient weather conditions. The remote stations can be 500 m from the central station or greater distances with line amplifiers. All power to the remote stations is supplied by the central station. The remote stations interface with transducers which generate the data to be recorded.

A remote station is connected to the central station via a cable containing three shielded twisted pairs. The remote station is addressed by a self-clocking 10-bit serial binary word generated by the central station. The remote station then senses the addressed channel and generates a 33-bit serial word which is transmitted to the central

station. Several types of data can be accepted by the remote station:

Analog, up to 160 channels per remote station, in any combination of high- or low-level signals (±10 mV to ±10 V full scale) in 8-channel increments, each

Digital, up to 16 channels of eight-digit 1248 binary-coded decimal (BCD) and up to 4 channels of eight-digit 1224 BCD, making a total of 20 channels per remote station.

Frequency, up to 10 channels per remote station in any combination of 1 Hz to 1 MHz or 100 Hz to 2 MHz, each range having an input sensitivity of 100 mV rms.

Contact Closure, up to 112 per remote station in groups of 8 per address.

The central station provides random access and flexibility in output format, automatically and manually interrogates the remote station, formats the data into 2048 character records, and writes the records on magnetic tape. The magnetic tape unit has the capability of read-after-write for checking that the data are being recorded correctly. The central station includes a real-time clock (days, hours, minutes, seconds) with crystal time base, as well as the capability of using an externally generated time code. The scan cycle rate is adjustable from 1 minute (or less if the total channel capacity is not fully used) to 24 hours.

Ten thumb wheels are provided on the front panel of the central station for reference data which are recorded in every record. A slow-speed paper printer allows operators to check the data being recorded on the magnetic tape. This printer is used for temporary, intermittent paper record of time selected data only, and is independent of the magnetic record. A visual display of time and any manually selected channel is provided in digital form on the central station. This display is independent of the operation of both the paper and magnetic records.

Each record written on the magnetic tape consists of as many data words as there are channels in operation plus header words. The header words are: (1) reference data selected by the thumb wheels on the central station, number of remote stations in operation, etc., and (2) the time code. Each data word is tagged with the remote station identification number and channel number.

All input channel signal conditioning is modularized so that a remote station has minimum configuration without excessive unused channels. Expansion of a remote station to maximum input channel configuration is by the addition of plug-in modules with no wiring changes required.

An uninterruptible power source maintains the system in full operation during momentary line power failures. A fully implemented system (ten remote stations) will operate for at least ten minutes without regular line power.

III. Recording Accuracy

One objective in the design of the data acquisition system was to make the errors in data transmission and recording insignificant in comparison with the inherent uncertainty in a wide variety of measuring sensors. A typical hemispherical pyranometer has an accuracy of about ±3%. The tracking heliometers, described below, have a specified accuracy of ±2%. The overall accuracy of the data system is of the order of 0.1%.

Figure 1 shows a block diagram of the data system.[1] The sensors detect a variety of physical parameters and convert the measurements to electrical signals which appear at the sensor's output terminals. Certain key parameters are recorded in analog form on strip chart recorders for immediate visual checking and comparisons. The diagram shows that some parameters are recorded in digital form, some as a frequency, and the remainder in analog form. The digital recording chain is the most precise, the standard method is the direct analog chain, and the frequency technique is intermediate between these two. The voltage-to-frequency converters are used for precise integration and accuracy in recording. If resistance–capacitance (RC) time constants are used for integration, then components with high stability and high precision must be used. Furthermore, integration times are limited to about 10 seconds with RC circuits because of the large values of the components. The voltage-to-frequency (V/F) conversion is a convenient method of providing accurate and flexible integration times. The input impedance for the V/F converters is of the order of 50 to 100 megohms and these devices will over-range to 2.5 times. The output from the V/F converters is 0 to 100 kHz for an input of 0 to 10 mV. Internal noise was measured as about 20 Hz in 100 kHz. The temperature coefficient is ±0.005% per °C (0 to 55°C).

[1]The multiplexer and data recording system were supplied by Instrumentation Technology Corporation of California.

Data which enter the SMDAS in frequency form allow integration by plug-in counter boards in the data system. Integration times of 0.1, 1, 10, 100, 1000 seconds are available in the system as well as 1, 2, 4, and 8 minutes.

Variable integration times are available in the high-precision chain shown in Fig. 1. The V/F output is fed into a computing counter and programmer pair, and the digital output is recorded directly in the SMDAS. The output from the programmer is digital BCD data in 5 significant figures. The computing counter is the Hewlett-Packard Model 5360A, whose frequency measurement accuracy is given by

$$\frac{10^{-9}}{\text{Count start/stop time}} \pm \text{trigger error} \pm \text{time base error}$$

The trigger error is inversely proportional to signal amplitude and is negligible except for very noisy or very-low-frequency signals, conditions which do not apply in this application. The built-in time base has a specification of 5 parts in 10^{11} for a 1-second averaging time. The overall accuracy of the frequency count is better than 0.01% for all possible conditions. In addition to providing variable integration times, the programmer is capable of inserting scaling factors, unit conversions or data calibrations, as required. Preprocessing of certain high data volume parameters can also be carried out by the computing counter–programmer combination, as described below.

Special attention has been paid to the accuracy of the transfer of signals from the various sensors to the input terminals of the data system. Typical output signals from the sensors are dc voltages in the range of 0 to 10 mV. The Spectrolab hemispherical pyranometer, for example, has an output of 7 mV per kW/m^2 insolation input. If the sensors are located more than a meter or two from the data system input, then the transmission line is subject to interference, line noise, ground loops, attenuation errors, etc. If amplifiers are used to boost the sensors' output to a level where these problems are suppressed, then the amplifiers are subject to temperature changes with the ambient environment. The Jet Propulsion Laboratory's experience over many years of building highly stabilized amplifiers has been used in designing and constructing suitable amplifiers and enclosures. Amplifiers with a gain of approximately 1000 are in use at Goldstone with accuracies of 0.5% (output) over an ambient temperature change of 100°C, and with accuracies of 0.01% (output) over the same ambient temperature range for oven-stabilized designs.

IV. Calibration

Calibration procedures depend on the parameter under investigation and on the type of sensor and measurement method. The calibration of microwave parameters has been discussed in the open literature (Refs. 4, 5, and 6) and in JPL reports (Refs. 7 and 8). In this report the calibration of two solar energy instruments will be discussed.

A typical pyranometer in the JPL solar measurement program is the Spectrolab Hemispherical Pyranometer, Model SR-75. Figure 2 shows the traceability of the calibration of this instrument to the World Radiation Center in Davos, Switzerland.

In addition to pyranometers, the JPL solar measurement program operates tracking heliometers. The heliometer is the Mark 3 Kendall Solar Radiometer System. This radiometer is almost identical with the primary absolute cavity radiometer, designed and built at JPL, and which has been described in the technical literature (Refs. 9 and 10). The only differences between the Mark 3 radiometer system and the primary absolute cavity radiometer (known as PACRAD) is the view angle which is 15 degrees instead of 5 degrees, and the flat quartz lens covering the aperture for all weather operation. The quartz lens contributes an attenuation of approximately 5%, which is not present in the PACRAD. The Mark 3 radiometers at Goldstone, both with and without the quartz lens, have been extensively calibrated against the PACRAD, which has itself undergone intercomparisons at the World Radiation Center at Davos, Switzerland (Ref. 10).

The Mark 3 radiometer system is a cavity-type radiometer with provisions for self-calibration. Figure 3 is a photograph of the system. The radiometer is designed for tracking and measuring solar irradiance. It is intended for use in outdoor environments in the Mojave area. It is compensated for changes in ambient temperature and is relatively insensitive to wind and rain. It has been designed to operate unattended over long periods of time (one or two months) in remote locations. In addition to the original calibration of the Mark 3 radiometer against the Kendall Mark 6 PACRAD absolute standard, it is also calibrated by correlating its output with an internally heated cavity. This allows subsequent calibrations to be made using a known applied voltage and current. These calibrations are checked periodically and program plans call for an annual recalibration against the PACRAD standard.

V. Examples of Computed Results

In order to demonstrate the flexibility and recording capability of the programmer chain in Fig. 1, some examples of wind data will be presented. Wind speed is measured at DSS 13 by a cup anemometer located at the top of a 30-m tower. The output from the anemometer was fed through a V/F converter and into the data system via a computing counter and programmer as shown in Fig. 1.

Two parameters of wind velocity are of interest to investigators of wind energy systems. These two parameters are: (1) the ratio of the mean of the cubes of wind velocity to the cube of the means of wind velocity over short periods of time, such as 2 minutes, as a function of wind velocity, and (2) the standard deviation of wind velocity over the same short periods as a function of wind velocity.

Wind speed was sampled and digitized at a 1-ms rate for a period of two minutes, less computation time and time taken to write a record on the magnetic tape. If the wind speed measurements in the 2-minute period are denoted V_i, then the following computations were performed by the computing counter–programmer combination:

$$\overline{V} = \frac{1}{N} \Sigma V_i \tag{1}$$

$$\overline{V^3} = \frac{1}{N} \Sigma (V_i)^3 \tag{2}$$

where N is the number of wind speed samples in the 2-minute period. In addition to these two computations, the standard deviation σ_V of the set of V_i measurements was calculated, and the peak value of V_i, $\hat{V}$ was found.

The following data were recorded on magnetic tape for each 2-minute period: Mean velocity $\overline{V}$, mean of the cubes $\overline{V^3}$, standard deviation of wind velocity σ_V, and peak wind velocity $\hat{V}$. From these recorded data it was possible to plot the ratio $\overline{V^3}/(\overline{V})^3$ as a function of $\overline{V}$, or any other combination of parameters of interest. Two 24-hour periods were chosen as representative examples. The first period was 2130 (PST) August 16 to 2200 (PST) August 17, 1975, when wind speeds of up to 16 m/s (about 35 mph) were experienced, and the second period was 0000 to 2400 (PST) September 13, 1975, which was a relatively calm period. Figure 4 shows a plot of the ratio of the mean of the cubes to the cube of the means of wind velocity ($\overline{V^3}/(\overline{V})^3$) as a function of mean wind velocity in each 2-minute period for August 16/17. There are as many data points plotted as there are 2-minute periods in this time range. A third-order curve has been fitted to the data to show the trend. Figure 5 shows a similar plot (to the same scales as Fig. 4) for the calm period, September 13, also with a third-order curve fitted to the data. Figure 6 is the same as Fig. 5, except the abscissa has been expanded. Figure 7 is a graph of the standard deviation of wind velocity in each 2-minute period against mean wind velocity in the same 2-minute periods for August 16/17, 1975. Here, again, there are as many data points plotted as there are 2-minute periods in this time span. A straight line has been fitted to the data to show the trend. Figure 8 is a similar plot for September 13, 1975.

VI. Conclusion

A flexible and versatile data acquisition system has been provided at Goldstone. It is capable of recording a wide variety of parameters from widely separated geographical locations with varying integration times and recording speeds. It is fast, accurate, and expandable to a maximum of 1600 analog channels plus 200 digital channels, plus 100 frequency channels, plus 1120 contact closures. It has demonstrated satisfactory operation by recording meteorological, microwave, solar energy, wind, and ionospheric data. Satisfactory operation in conjunction with preprocessing equipment or microprocessors has also been demonstrated.

References

1. Reid, M. S., and Lockhart, T. J., "The Variation of Atmospheric Temperatures at Microwave Frequencies," Conference Record of *Conference on the Propagation of Radio Waves at Frequencies about 10 GHz*, London, England, Apr. 1973.

2. Reid, M. S., "Tracking and Ground Based Navigation: A Description of the Weather Project," in *The Deep Space Network Progress Report*, Technical Report 32-1526, Vol. X, pp. 116–122, Jet Propulsion Laboratory, Pasadena, Calif., Aug. 15, 1972.

3. Reid, M. S., Gardner, R. A., and Parham, O. B., "Goldstone Solar Energy Instrumentation Project: Description, Instrumentation, and Preliminary Results," in *The Deep Space Network Progress Report 42-26*, pp. 133–144, Jet Propulsion Laboratory, Pasadena, Calif., Apr. 15, 1975.

4. Stelzreid, C. T., and Reid, M. S., "Precision Power Measurements of Spacecraft CW Signal Level with Microwave Noise Standards," *Trans. IEEE, Instrumentation and Measurement*, Vol. IM-15, No. 4, pp. 318–324, Dec. 1966.

5. Stelzried, C. T., "A Liquid Helium Cooled Coaxial Termination," *Proc. IRE*, Vol. 49, No. 7, p. 1224, July 1961.

6. Stelzried, C. T., "Temperature Calibration of Microwave Thermal Noise Sources," *Trans. IEEE, Microwave Theory and Techniques*, Vol. MTT-13, No. 1, p. 128, Jan. 1965.

7. Reid, M. S., and Stelzried, C. T., "Error Analysis of CW Signal Power Calibration with Thermal Noise Standards," in *Supporting Research and Advanced Development*, Space Programs Summary 37-36, Vol. IV, pp. 268–277, Jet Propulsion Laboratory, Pasadena, Calif., Dec. 31, 1965.

8. Reid, M. S., "Improved RF Calibration Techniques: System Operating Noise Temperature Calibrations of Low Noise Cones," in *The Deep Space Network*, Space Programs Summary 37-66, Vol. II, pp. 57–61, Jet Propulsion Laboratory, Pasadena, Calif., Nov. 30, 1970.

9. Kendall, J. M., Sr., *Primary Absolute Cavity Radiometer*, Technical Report 32-1396, Jet Propulsion Laboratory, Pasadena, Calif., July 15, 1969.

10. Frohlich, C., "The Third International Comparisons of Pyrheliometers and a Comparison of Radiometric Scales," *Solar Energy*, Vol. 14, No. 2, pp. 157–166, 1973.

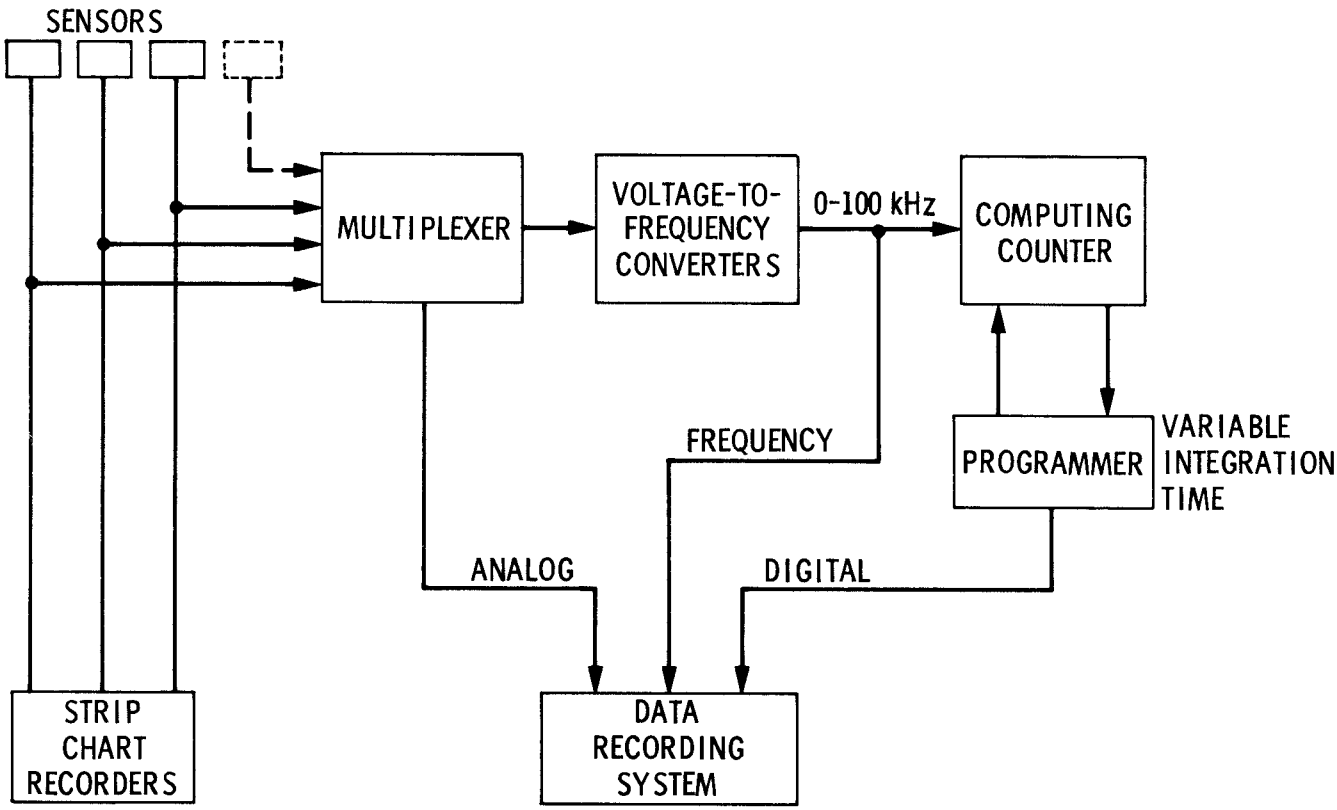

Fig. 1. Block diagram of the data acquisition system

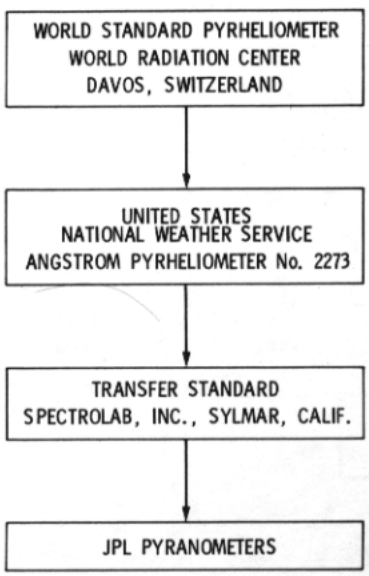

Fig. 2. Traceability of the calibration of JPL pyranometers

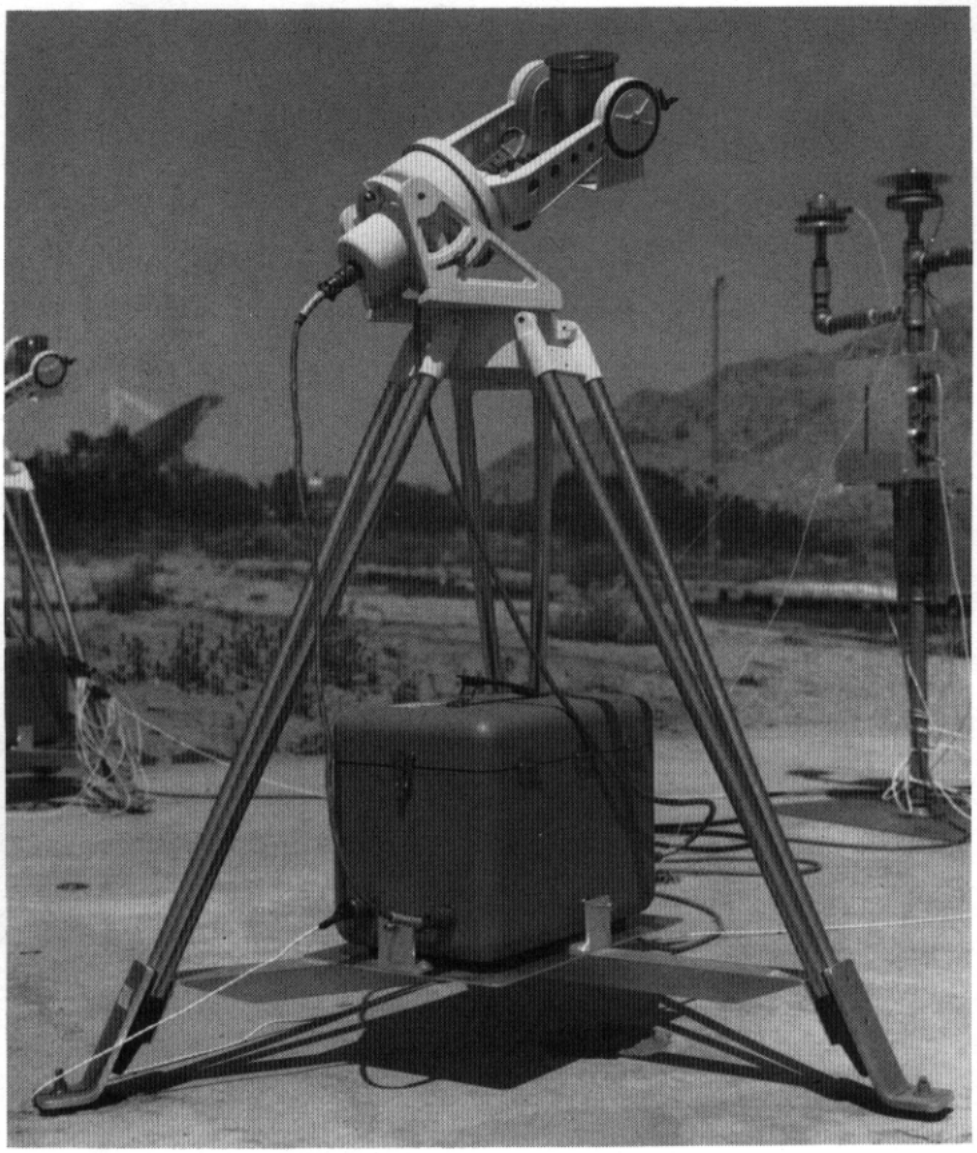

Fig. 3. The Mark 3 Kendall Solar Radiometer System

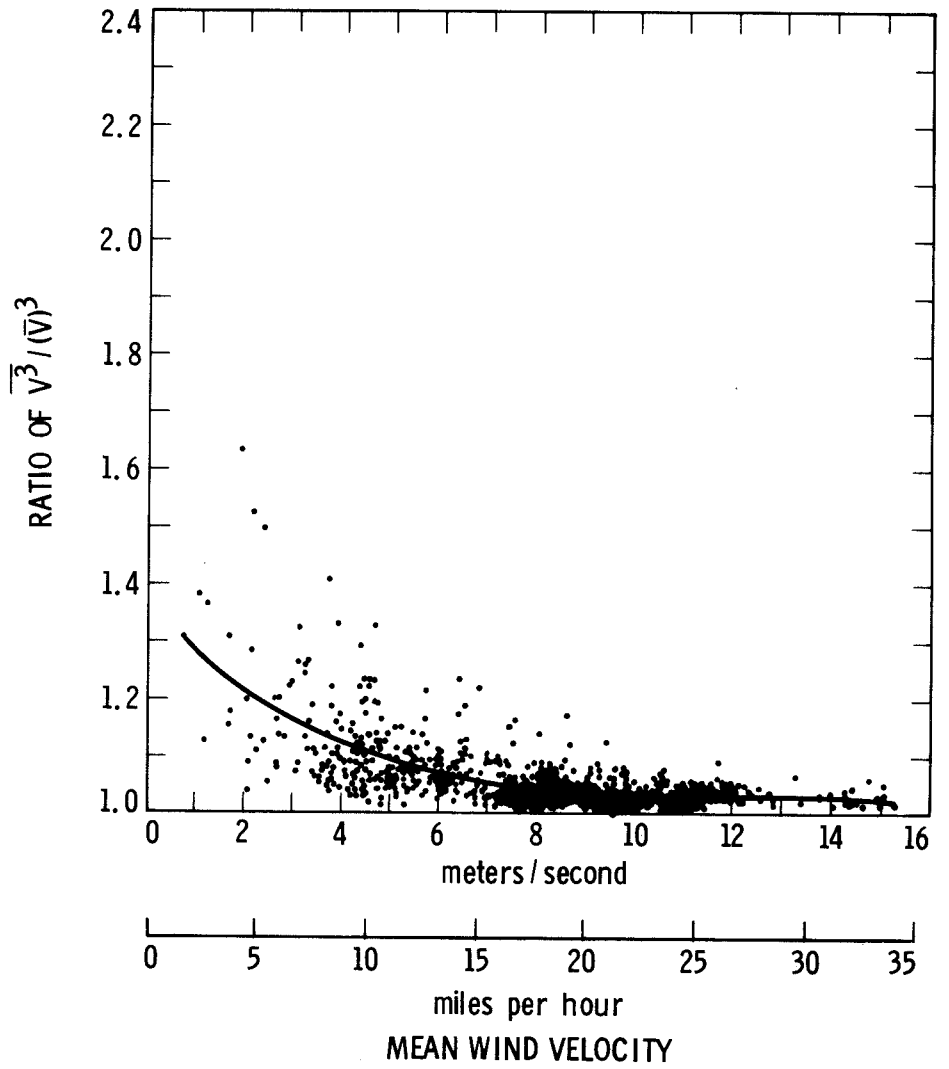

Fig. 4. Ratio of $\overline{V^3}/(\bar{V})^3$ as a function of mean wind velocity for August 16/17, 1975 measured at Goldstone

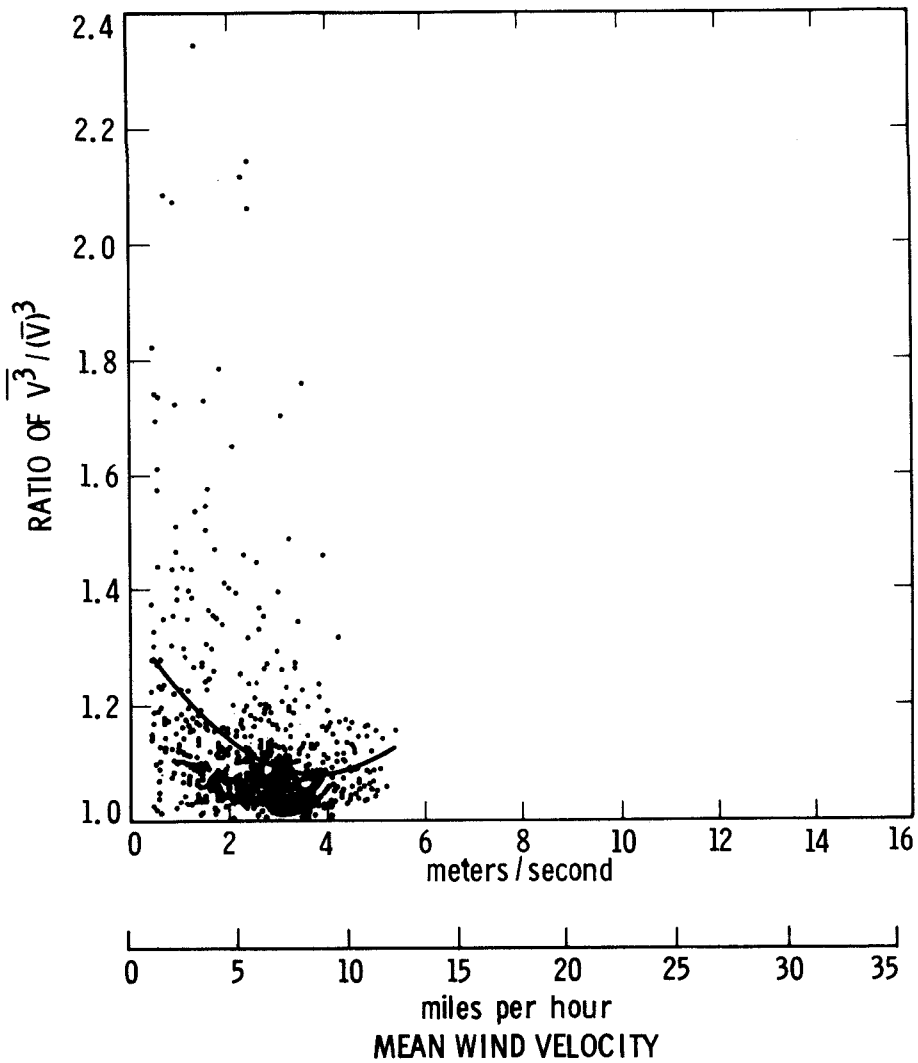

Fig. 5. Ratio of $\overline{V^3}/(\bar{V})^3$ as a function of mean wind velocity for September 13, 1975 measured at Goldstone

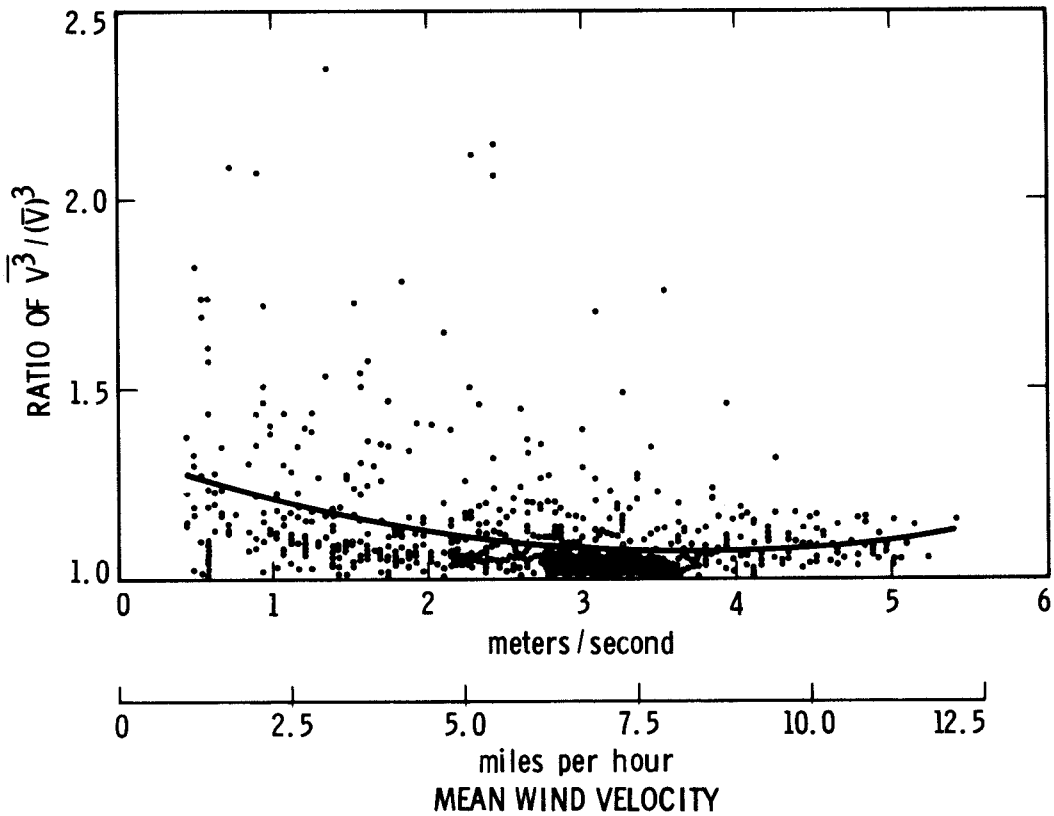

Fig. 6. Ratio of $\overline{V^3}/(\bar{V})^3$ as a function of mean wind velocity for September 13, 1975 on an expanded scale

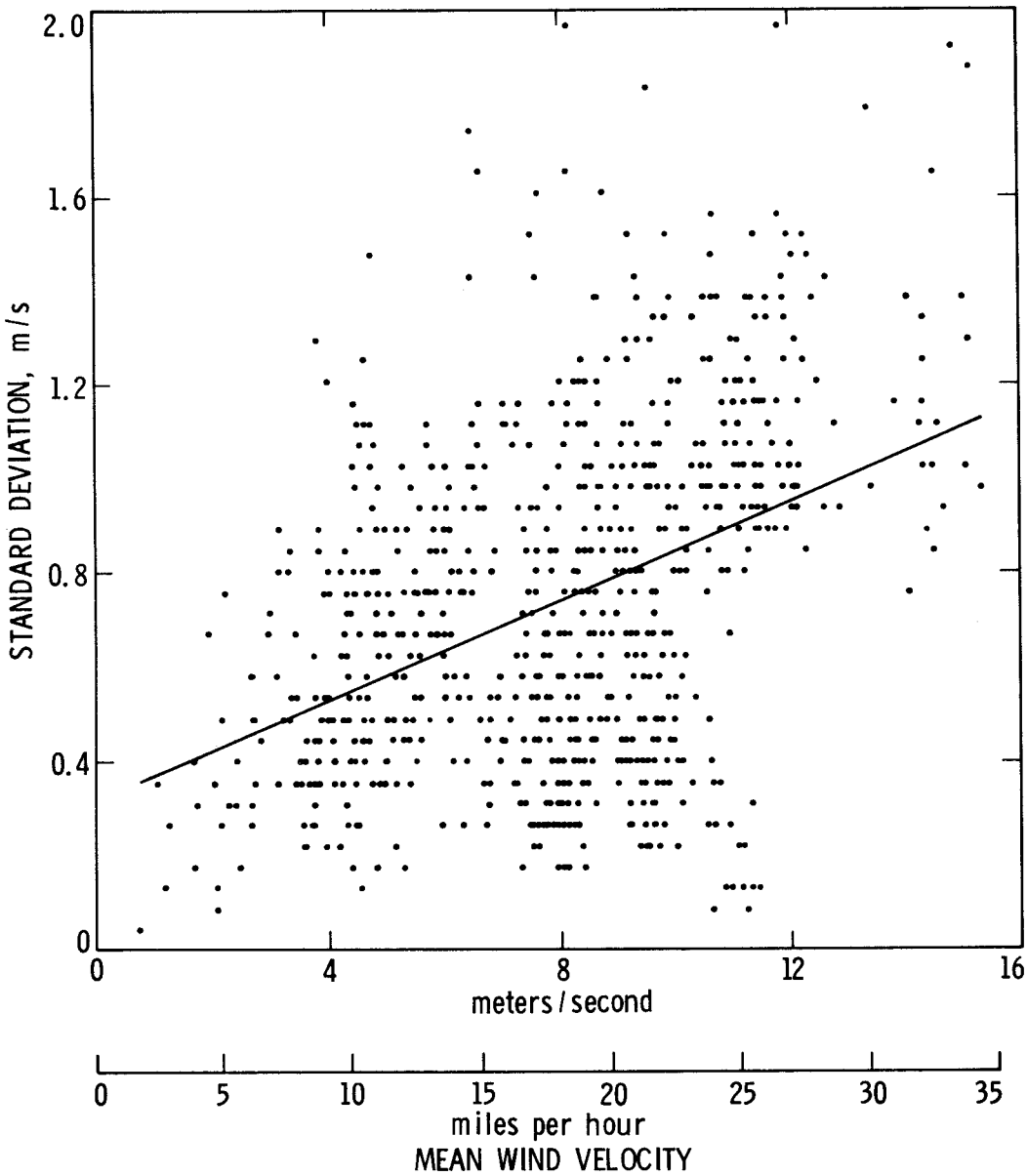

Fig. 7. Standard deviation of wind velocity as a function of mean wind velocity for August 16/17, 1975

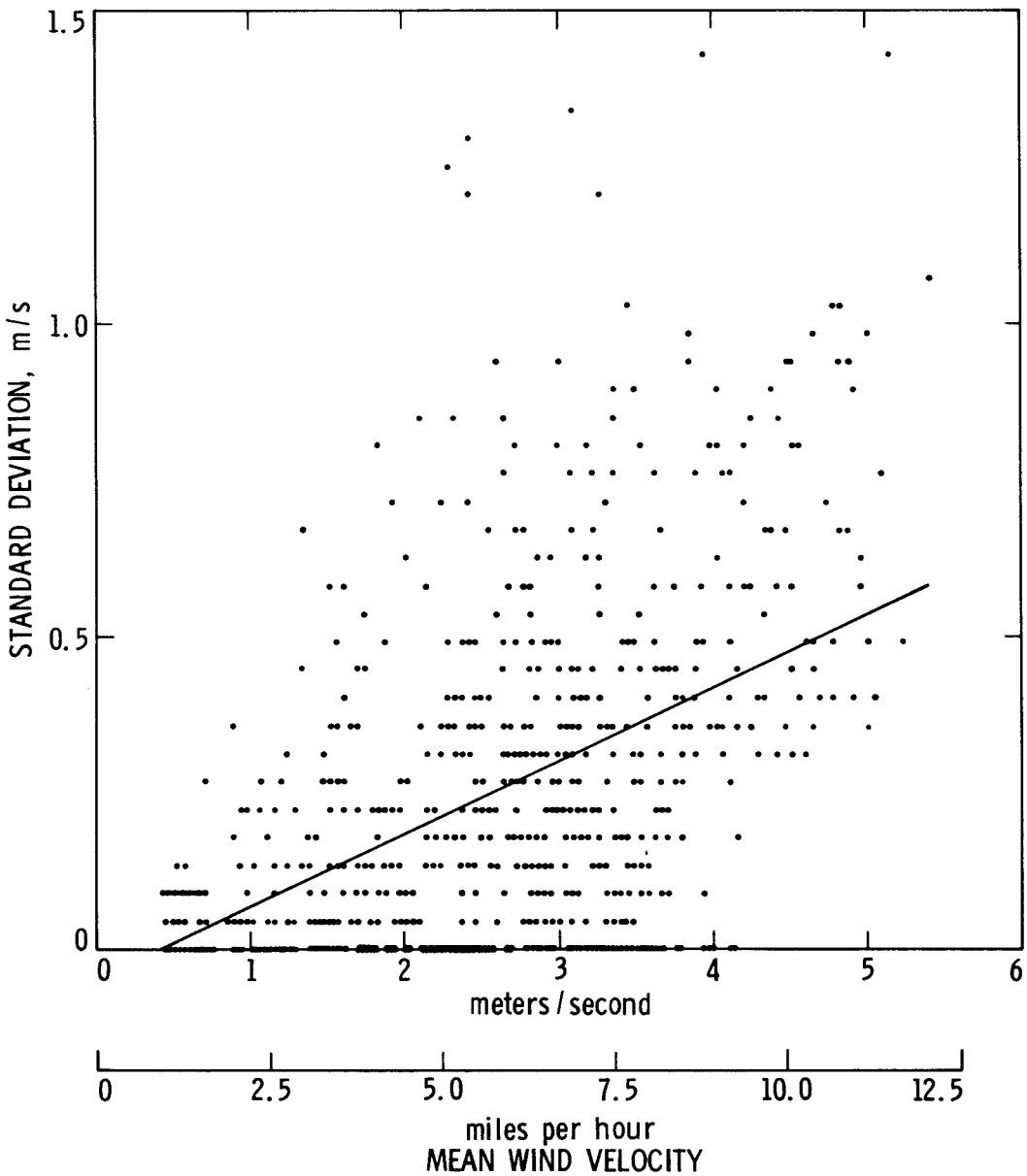

Fig. 8. Standard deviation of wind velocity as a function of mean wind velocity for September 13, 1975